

Distinctive character of electronic and vibrational coherences in disordered molecular aggregates

Vytautas Butkus,^{1,2} Donatas Zigmantas,³ Darius Abramavicius,^{1,4} Leonas Valkunas,^{1,2}

¹*Department of Theoretical Physics, Faculty of Physics,*

Vilnius University, Sauletekio 9-III, 10222 Vilnius, Lithuania

²*Center for Physical Sciences and Technology, Gostauto 9, 01108 Vilnius, Lithuania*

³*Department of Chemical Physics, Lund University, P.O. Box 124, 22100 Lund, Sweden and*

⁴*State Key Laboratory of Supramolecular Complexes, Jilin University,*

*2699 Qianjin Street, Changchun 130012, PR China**

Coherent dynamics of coupled molecules are effectively characterized by the two-dimensional (2D) electronic coherent spectroscopy. Depending on the coupling between electronic and vibrational states, oscillating signals of purely electronic, purely vibrational or mixed origin can be observed. Even in the “mixed” molecular systems two types of coherent beats having either electronic or vibrational character can be distinguished by analyzing oscillation Fourier maps, constructed from time-resolved 2D spectra. The amplitude of the beatings with the electronic character is heavily affected by the energetic disorder and consequently electronic coherences are quickly dephased. Beatings with the vibrational character depend weakly on the disorder, assuring their long-time survival. We show that detailed modeling of 2D spectroscopy signals of molecular aggregates provides direct information on the origin of the coherent beatings.

INTRODUCTION

Dynamic properties of electronic excitations in artificial and biological molecular aggregates depend on the intra- and inter-molecular interactions. Due to resonant intermolecular interactions, electronic excitations of the aggregate form collective exciton states exhibiting coherent relationship between molecular excited states [1, 2]. Interactions with intramolecular vibrations reflect the specificity of molecular constituents of the aggregate and usually manifest themselves as vibrational sub-bands in electronic absorption or fluorescence spectra. Depending on the relative strength of these interactions, the induced excitations in molecular aggregates may lead to a host of photoinduced dynamics: from coherent and incoherent energy migration to reorganization of the surrounding environment [3–6].

To resolve the details of the excitation evolution many time-resolved techniques have been developed and the most recent of them is the femtosecond coherent two-dimensional (2D) spectroscopy [7, 8], which has been applied in studies of various molecular aggregates, e. g. photosynthetic pigment-protein complexes, polymers, tubular aggregates, quantum dots [9–14]. These studies have shown the inherent complexity of the 2D spectra. For instance, the long-lasting oscillatory features, initially attributed to electronic quantum coherences, have been resolved [11, 12, 15, 16]. Possible vibronic origin of some of these beats has been proposed in a number of recent studies [17–21]. Coupling to multiple intramolecular vibrational modes is essential for the spectral properties of the most chromophore molecules and it can introduce complex effects to the 2D spectra.

Since the role of the coherence is considered to be an important factor for defining the excitation dynamics in

molecular aggregates the task of distinguishing electronic and vibrational character of coherences is essential and at the same time very challenging issue. To distinguish between the origins of the spectral oscillating behavior a molecular dimer as the simplest vibronic molecular aggregate model is considered. This work is an extension of our previous comparative study of coherent 2D spectra of vibrational monomer and electronically-coupled dimer [17]. Here we demonstrate that coherent oscillations of electronic and vibrational character are mixed due to intermolecular interactions. However, they exhibit distinct oscillation maps and different behavior with respect to the energetic disorder and, thus, can be discriminated in the 2D spectra.

MODEL

As usual for resonant spectroscopy applications let us assume that a constituent chromophore molecule of the aggregate is characterized by two levels corresponding to electronic (ground and excited) states. Let us also assume that the electronic transitions are coupled to a single nuclear coordinate of high-frequency intramolecular vibration ω_0 . This coupling can be effectively represented in terms of the displaced harmonic oscillator model [22, 23]. The electronic excitation results in the shift along the dimensionless coordinate q of the potential energy surface defined in the ground state as $V(q) = \hbar\omega_0 q^2/2$. If the Heitler-London approximation is assumed [1, 2] the Hamiltonian of the dimer is then

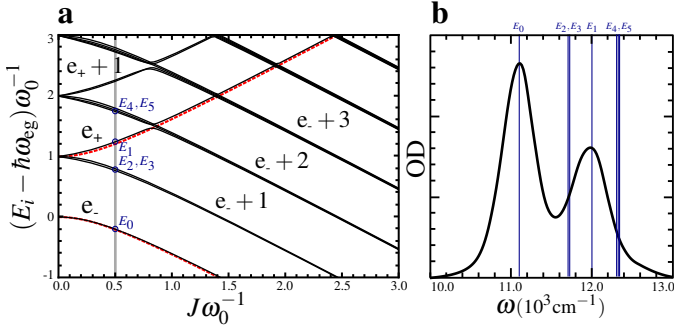


FIG. 1. Dependence of the eigen energies of the molecular dimer on the resonant coupling (a, black solid lines) in the case of small Huang-Rhys factors, i.e. $s_1 = s_2 = 0.05$. A clear separation of electronic excited states (denoted as e_- and e_+ , respectively) and vibronic states (denoted as $e_{\pm} + m$, where m – the number of vibrational quanta) is observed. The eigen energies of a purely electronic dimer $E_{e_{\pm}}$ (by setting the Huang-Rhys factors to zero) are represented by the red dashed lines. (b) The absorption spectrum of the molecular vibronic dimer with coupling $J = 0.5\omega_0$ is also shown, which corresponds to the energy states indicated by the vertical gray line in (a). Positions of the transitions contributing to the absorption spectrum are indicated by vertical lines.

given by

$$\begin{aligned} \hat{H} = & T + [V(q_1) + V(q_2)] |g\rangle\langle g| \\ & + [\varepsilon_1 + V(q_1 - d_1) + V(q_2)] |e_1\rangle\langle e_1| \\ & + [\varepsilon_2 + V(q_1) + V(q_2 - d_2)] |e_2\rangle\langle e_2| \\ & + J [|e_1\rangle\langle e_2| + |e_2\rangle\langle e_1|] \\ & + [\varepsilon_1 + \varepsilon_2 + V(q_1 - d_1) + V(q_2 - d_2)] |f\rangle\langle f|, \quad (1) \end{aligned}$$

where $|g\rangle$ is the electronic common ground state, $|e_n\rangle$ ($n = 1, 2$) corresponds to the electronic excited state of the n -th chromophore of the dimer, when the other remains in the ground state; $|f\rangle$ is the doubly-excited state of the dimer, which corresponds to electronic excitations of both monomers. Term T represents the total kinetic energy of the vibrational harmonic oscillators coupled to both molecules, $T \equiv T_1 + T_2$, d_n is the displacement value of the vibrational potential in the electronically excited state and ε_n is the energy difference between the $|g\rangle$ and $|e_n\rangle$ states potential minima of the n -th monomer, J is the resonance interaction. Since $V(q_n - d_n) - V(q_n) = \lambda_n - \hbar\omega_0 d_n q_n$ with $\lambda_n = \hbar\omega_0 d_n^2/2$ being so-called reorganization energy, this difference in the potential energies determines the coupling of the electronic excitation to molecular vibrations. The latter is usually characterized by the dimensionless Huang-Rhys factor $s_n = d_n^2/2$.

In the case of no displacement ($s_1 = s_2 = 0$) the electronic excitations are not coupled to molecular vibrations and the electronic part of the Hamiltonian is easily diagonalized giving exciton eigen energies of an electronic dimer, $E_{e_{\pm}} = \hbar\omega_{eg} \pm \Delta E_{ED}$, where $\omega_{eg} = \frac{1}{2}(\varepsilon_1 + \varepsilon_2)$ and

$\Delta E_{ED} = \frac{1}{2}\sqrt{(\varepsilon_2 - \varepsilon_1)^2 + 4J^2}$. Dependence of the exciton energies of electronic dimer on the coupling is shown in Fig. 1a by the red dashed lines. The remaining vibrational Hamiltonian is the harmonic oscillator which can be easily quantized.

The ground-state Hamiltonian is diagonal by definition (the Hamiltonian is defined in the basis of the electronic ground state) independently on the value of s_n and contains a ladder of vibrational states with energies spaced by $\hbar\omega_0$. A very similar result is also obtained for the single exciton block of the Hamiltonian (Eq. 1), which is, however, dependent on the value of s_n . After numerical diagonalization, if a sufficient number of vibrational states ν_{vib} is taken into account the excitation energies are found approximately at $E_{e_{\pm}} + \hbar\omega_0 m$ and $E_{e_{\pm}} + \hbar\omega_0 m$ ($m = 0, 1, \dots$) and constitute two ladders of equally-spaced states, denoted by $e_{\pm} + m$ and $e_{\pm} - m$ in Fig. 1a. In calculations, a deviation from this ladder structure for the higher energy states depends strongly on the number ν_{vib} of included vibrational levels.

In the frame of Heitler-London approximation we denote the electronic ground state as the state where both molecules are in their ground states with arbitrary vibrational excitations, $|g_i g_j\rangle$. Index i indicates the i -th vibrational excitation of the first molecule and j denotes the vibrational excitation of the second molecule. $|e_i\rangle = |e_i g_j\rangle$ denotes the state of the first molecule being in the electronic excited state maintaining the i -th vibration quantum and the second molecule being in the j -th vibrational ground state; analogously, $|e_2\rangle = |g_i e_j\rangle$ corresponds to the state where the second molecule is electronically excited. Doubly-excited electronic states $|f\rangle = |e_i e_j\rangle$ are constructed in a similar way. In terms of these definitions the vibronic set of eigenstates for the singly- and doubly-excited electronic states (state vectors $|u\rangle$ and $|v\rangle$, correspondingly) can be obtained by using the relevant transformations $|u\rangle = \sum_{ij} (\phi_{u,e_i g_j}^{(1)} |e_i g_j\rangle + \phi_{u,g_i e_j}^{(2)} |g_i e_j\rangle)$ and $|v\rangle = \sum_{ij} \Phi_{v,e_i e_j} |e_i e_j\rangle$. The corresponding transformation coefficients $\phi^{(n)}$ and Φ are acquired from the diagonalization of the singly-excited and doubly-excited blocks of the Hamiltonian, Eq. (1) and provide us with the information about the eigenstate composition and allow us to estimate the amount of mixing between vibrational and electronic states.

The transition dipole moments between the ground and singly-excited states as well as between singly- and double-excited states in vibronic eigenstate basis are then given by

$$\mu_{u,g_i g_j} = \mu_1 \phi_{u,e_i g_j}^{(1)} + \mu_2 \phi_{u,g_i e_j}^{(2)} \quad (2)$$

and

$$\mu_{v u} = \mu_2 \sum_{ijlm} \phi_{u,e_l g_m}^{(1)} \Phi_{v,e_i e_j} + \mu_1 \sum_{ijlm} \phi_{u,g_i e_m}^{(2)} \Phi_{v,e_i e_j}, \quad (3)$$

where μ_1 and μ_2 are the transition dipole moments of the monomers.

Further on we will consider 2D signals, which are calculated using the perturbative system-response function theory in the vibronic eigenstate basis using the impulsive limit of the laser pulses, i.e. assuming that the laser pulse spectrum covers all frequencies. More information regarding the details of calculations can be found elsewhere [24, 25]. For the sake of simplicity, we assume the pure dephasing as the only mechanism responsible for the homogeneous lineshape formation. The energetic disorder (uncorrelated fluctuations of site energies ε_n) is considered to be responsible for the inhomogeneous broadening that is taken into account by averaging over ensemble (1000 realizations of independent simulations) with the Gaussian distribution with standard deviation σ_D of excitation energies for every monomer.

RESULTS

We consider the molecular dimer for which the Huang-Rhys factors are equal for both monomers, $s \equiv s_1 = s_2$. We set vibrational frequency ω_0 as the reference parameter and assume the resonant coupling strength $J = -\omega_0/2$. The electronic site energies are separated by the same value as vibrational frequency, $\varepsilon_2 - \varepsilon_1 = \omega_0$, and in the case of small values of the Huang-Rhys factors the excitonic energy gap ΔE_{MD} is approximately equal to the excitonic splitting of the electronic dimer ($\Delta E_{MD} \approx \Delta E_{ED}$). As values typical for aggregates, we consider $\omega_0 = 600 \text{ cm}^{-1}$ and $s = 0.05$, thus resulting in $\Delta E_{MD} \approx 867 \text{ cm}^{-1}$. Hence, the excitonic splitting is off-resonant from the vibrational resonance (see Fig. 1a). We assume that the strengths of the transition dipole moments of the monomers are equal and constitute the inter-dipole angle $\varphi = \frac{3\pi}{5}$. The dephasing rate determining the homogeneous linewidth is chosen to be $\gamma = \omega_0/6$ and central absorption frequency - $\omega_{eg} = 11500 \text{ cm}^{-1}$. These parameters are similar to the ones used in our previous publication [17]. For numerical calculations we choose $\nu_{\text{vib}} = 8$, as calculations with more vibrational states show no evident changes in any simulated spectroscopic signals for the used set of parameters. A smaller number vibrational states (e.g. $\nu_{\text{vib}} = 2$) results in a significantly irregular distribution of vibronic state energies [21]. Even when sufficient number of vibrational states is included, deviation from a harmonic ladder of vibronic states appears due to non-trivial repulsion between isoenergetic vibrational states. However, this effect is insignificant for the model considered here, as the eigen energy departure from ideal harmonic progression is less than 5% for the parameters used.

The exciton interactions with the vibrations are almost indistinguishable in the absorption spectrum for the chosen small value of the Huang-Rhys factor $s = 0.05$ as the

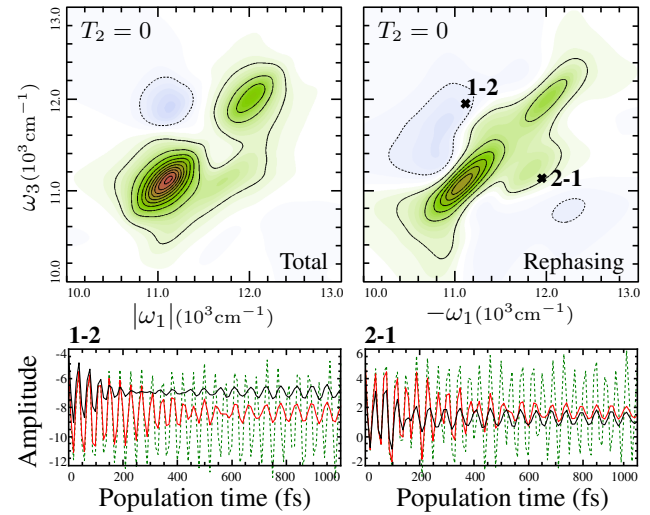


FIG. 2. The total (a sum of rephasing and non-rephasing) and rephasing 2D spectra of the molecular dimer at the population time $T_2 = 0$, with Gaussian disorder $\sigma_D = 200 \text{ cm}^{-1}$ (upper panels). Solid (dashed) contour lines for positive (negative) signals are drawn in 10% intervals. Time dependence of the amplitudes of the upper (1-2) and lower (2-1) cross-peaks of the rephasing signal are shown in the lower panels (left and right, respectively). Green – no disorder, red – $\sigma_D = 20 \text{ cm}^{-1}$, black – $\sigma_D = 50 \text{ cm}^{-1}$.

only evidence of vibronic character is a sole weak shoulder in absorption at $\sim 12600 \text{ cm}^{-1}$ (Fig. 1b). For the larger Huang-Rhys factors the deviation from the harmonic ladder becomes significant, especially close to the resonance conditions, when electronic splitting matches vibrational quantum (see Fig. 1a). In this case strong vibrational progression would evidently appear in the spectrum. However, the conclusions of further discussion would not change appreciably.

Transition amplitudes μ_{u,gig_j} between the ground state manifold of the vibrational states and the manifold corresponding to the singly-excited state signify possible interaction configurations. The "vibrational content" in a specific electronic transition can be quantified by the Franck-Condon factors combined as $\chi_u = \left(\phi_{u,gog_0}^{(1)} \right)^2 + \left(\phi_{u,gog_0}^{(2)} \right)^2$. The maximum value of this quantity ($\chi_u = 1$) reflects the pure electronic character of the eigenstate. Contributions of the transitions originating from the zero-vibrational state, i. e. $|g_0g_0\rangle$ are shown in Table I. The two most significant transitions correspond to electronic-only transitions with $\chi \geq 0.9$, while the other transitions are of vibronic origin with dominant vibrational character ($\chi < 0.1$).

Let us now inspect the total and rephasing 2D spectra shown in Fig. 2. These spectra feature three positive peaks: two diagonal peaks and a clearly distinguishable cross-peak (2-1) below the diagonal reflecting the coherent resonance coupling between the monomers. The

u	$E_u - E_0, \text{ cm}^{-1}$	μ_{u,g_0g_0}	χ_u	$\varphi_u, \text{ deg}$	States in site basis					
					$ e_0g_0\rangle$	$ g_0e_0\rangle$	$ e_1g_0\rangle$	$ g_0e_1\rangle$	$ e_0g_1\rangle$	$ g_1e_0\rangle$
0	0	1.08	0.96	19.0	0.82	0.14	0.03	0.00	0.00	0.00
1	867	0.84	0.90	-81.8	0.15	0.76	0.02	0.01	0.05	0.01
2	581	0.26	0.06	69.3	0.00	0.06	0.37	0.09	0.37	0.06
3	600	0.17	0.02	19.0	0.02	0.00	0.38	0.07	0.41	0.07
4	1467	0.13	0.02	-81.3	0.00	0.02	0.09	0.36	0.06	0.36
5	1480	0.11	0.01	69.8	0.00	0.01	0.08	0.33	0.08	0.36

TABLE I. Mixed character of the lowest vibronic eigenstates of the molecular dimer with the Huang-Rhys factor $s = 0.05$. Value of $\chi_u = 1$ signifies a completely electronic character of the exciton state, while $\chi_u = 0$ corresponds to the vibrational character. φ_u denotes the angle of corresponding transition dipole vector with respect to the electronic transition dipole of the first monomer. $E_u - E_0$ corresponds to the energy gap between vibronic states and μ_{u,g_0g_0} – to the transition dipole moment.

higher cross-peak (1-2) is less visible due to the overlap with the excited state absorption (ESA) contribution. The peaks are elongated along the diagonal line ($|\omega_1| = \omega_3$) due to the inhomogeneous disorder. Apparent simple structure of the spectra disguise the complicated pattern of various overlapping contributions. The multitude of them is illustrated in Fig. 3a (only oscillatory contributions are shown in the scheme). Time dependent traces of the upper (1-2) and lower (2-1) cross-peaks of the rephasing signal reveal oscillation dynamics, which is strongly affected by the disorder in the system (see Fig. 2, lower panels).

The temporal dynamics of all peaks can be sorted into: i) *stationary contributions*, denoting the Liouville pathways, where the aggregate is in a population state during delay time T_2 of either the single exciton manifold or the ground electronic state manifold; ii) *oscillating contributions*, denoting the Liouville pathways of the ground or excited state vibronic and electronic coherences. The oscillations can be characterized by studying the so-called oscillation Fourier maps which are constructed by applying the Fourier transform to the real part of the rephasing spectrum $S_R(\omega_3, T_2, \omega_1)$ with respect to the time T_2 [14, 15],

$$A(\omega_3, \omega_2, \omega_1) = \int_0^\infty dT_2 e^{i\omega_2 T_2} \text{Re}S_R(\omega_3, T_2, \omega_1). \quad (4)$$

This allows us to directly identify the phase and amplitude of oscillations in the different spectral regions. We consider the oscillation maps of the 2D spectra at frequencies corresponding to $\omega_2 = \omega_0$ and $\omega_2 = \Delta E_{\text{MD}}$. Note that the oscillation map of electronic-character coherences involving two lowest “mixed” states (see Table I) and oscillating at frequency ΔE_{MD} is the same as the purely electronic coherence map of an excitonic dimer [17], i.e. oscillations in the rephasing part appear only in the cross-peaks. The obtained oscillation maps for disorder values $\sigma_D = 0$ and $\sigma_D = 200 \text{ cm}^{-1}$ are presented in Fig. 3b and c, respectively. As we find in the inhomogeneously disordered system ($\sigma_D = 200 \text{ cm}^{-1}$) the oscillating patterns are completely dominated by the vibrational

frequency ω_0 , while the oscillations with the electronic gap frequency ΔE_{MD} are at least 20 times weaker and thus, their contribution is negligible. The oscillation map of disordered vibronic dimer is highly asymmetric, which is mostly due to the ground state bleaching (GSB) contribution (Fig. 3a).

It is known that the phase of spectral oscillations of the electronic-only systems is 0 at the maxima of the peaks and changes continuously when going away from the peak. For the monomer coupled to a single mode of high-frequency vibrations, the phase of either 0 or π can be obtained depending on the coupling strength [22]. However, in congested spectra any phase relationships can be obtained if the spectral overlap is substantial. Especially for the mixed system, when both resonance coupling and vibronic interactions are taken into account. For example, it can be seen in the oscillation map in Fig. 3c that at the center of the lower diagonal peak the phase is detuned to approximately $2\pi/3$ from the value of π , which would be expected for an isolated oscillating peak [18, 22].

DISCUSSION

The introduced model of molecular dimer captures both limiting cases of purely vibrational and purely electronic model systems considered previously [17]. Indeed, by assuming either the Huang-Rhys factors or the resonance interaction to be zero both limiting cases can be obtained. Two prominent frequencies are present in the simulated oscillatory dynamics of the 2D spectrum of the vibronic molecular system (see the time dependence of two main cross-peaks shown in Fig. 2). Evidently, one frequency corresponds to the electronic energy gap ΔE_{MD} , while the other is equal to the vibrational frequency ω_0 . Beating with electronic and vibrational character result in distinct oscillation maps and therefore the origin of the oscillation can be identified.

Strength of oscillations strongly depends on system inhomogeneity. From simulations, this can clearly be seen

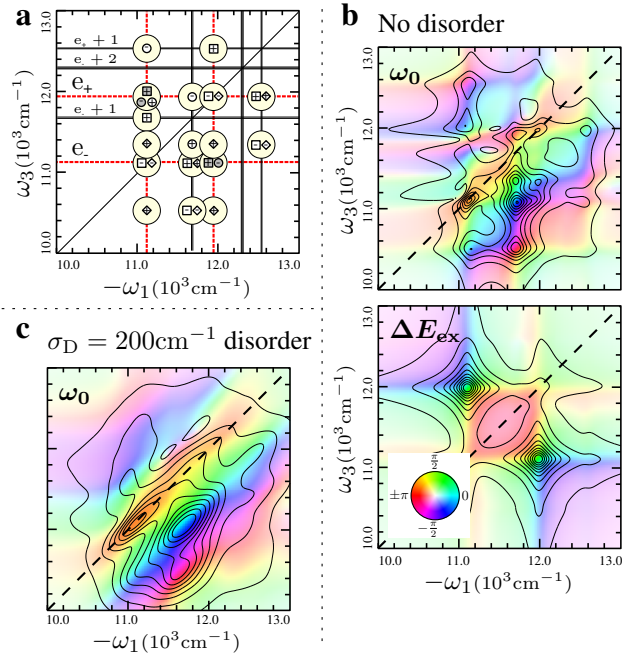


FIG. 3. (a) Arrangement of the the most significant (90% of the total amplitude) oscillatory contributions (diamonds denote GSB, squares – SE and circles – ESA) in the 2D spectrum of the molecular dimer. The oscillations are at vibrational frequency ω_0 (open symbols) or electronic frequency ΔE_{MD} (full gray symbols) and the plus/minus sign at each peak denotes the phase of the oscillation. (b) The Fourier maps are represented by the amplitude and phase of oscillations as contour lines and peak color, respectively, at frequencies ω_0 and ΔE_{MD} when $\sigma_D = 0$. (c) The oscillation map at frequency ω_0 when $\sigma_D = 200 \text{ cm}^{-1}$. The map at ΔE_{MD} frequency is not shown since it has negligible amplitude.

in the lower panel of Fig. 2, where time dependencies of the peak value for different values of the Gaussian disorder ($\sigma_D = 0, 20$ and 50 cm^{-1}) are presented. The initial intensive oscillations with the ΔE_{MD} frequency decay rapidly when the disorder is increased and the only dynamics observed at longer delay times correspond to the ω_0 beats. Strengths of the oscillations at different frequencies are represented by the corresponding values of the amplitude in the maps of the oscillations. Therefore, the value of amplitude maximum of the oscillation is used to evaluate its strength. The amplitude of electronic oscillations decays sharply with the disorder, while dependence of the amplitude of vibronic coherences is much more flat (the amplitudes for the stimulated emission (SE), ESA and GSB contributions are presented in Fig. 4). When disorder is absent, signatures of electronic coherences mostly coming from the SE contribution are at least 5 times larger than those of vibronic character, while for $\sigma_D > 200 \text{ cm}^{-1}$ the amplitude of electronic coherences is negligible (the corresponding oscillation map for $\sigma_D = 200 \text{ cm}^{-1}$ cannot be resolved).

Separation of coherences of electronic and vibrational

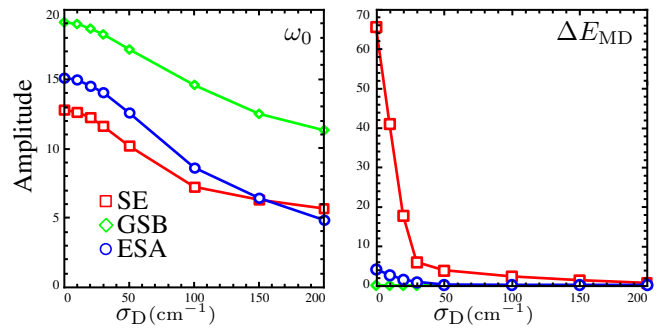


FIG. 4. Maximal amplitude of the oscillation, taken from the oscillation maps as a function of disorder for GSB (diamonds), SE (squares) and ESA (circles) contributions at different beating frequencies (ω_0 and ΔE_{MD}).

character is very significant as our results demonstrate that besides vibrational beats the electronic beats could be in principle observed and distinguished for the weakly disordered systems. However, the electronic beats rapidly decay in time in a Gaussian fashion (for the Gaussian disorder) as σ_D^{-1} . Whereas vibrational beats will prevail for longer times.

Note that in the Hamiltonian used (Eq. 1) no transformation of canonical variables into symmetric and antisymmetric components is performed that would allow us to decouple the Schrödinger equations of the excited and ground states. Therefore, presented model contains states which are not separated to diabatic or adiabatic ones as has been done in the theoretical work of Jonas and coworkers addressing coherences in FMO [18]. Also, since we show the separation of beats of electronic and vibronic character for arbitrary system parameters, the resonant condition of the mixed character coherences (i.e. when electronic energy gap is equal to the vibrational frequency) is just a special case of our model. It supports the assumptions about coherences in FMO where such resonant conditions are met – electronic coherences at initial times could be of the same order as those of the vibronic origin due to disorder of approximately 25 cm^{-1} ; electronic beats will decay in a short time ($\sim 200 \text{ fs}$) while vibrational beats would persist over the long time. For highly disordered systems (for example, chlorosomes) electronic coherences are not likely to be significant at all and the observed coherent dynamics are due to the ground-state vibrations [26].

It is important also to consider transition dipole moment orientations φ_u listed in Table I. The orientations of the transitions to the “mixed” states are different for each state and are also different from the transition dipole moments of monomer transitions. This implies that coherences involving arbitrary states (of electronic or vibrational character) will survive the measurements with polarization schemes, devised to suppress all but electronic coherence signals [16, 27]. On the other hand, these po-

larization schemes can then be used to distinguish between purely vibrational (localized on one molecule) and mixed origin coherences.

Results presented here are related to the assumption that the vibrational frequencies are not affected by inhomogeneities, which induce the disorder of electronic transition energy. This is often the case as vibrational resonances are less sensitive to the electrostatic configuration of the environment than the delocalized electronic wavefunctions. Vibrational coherences, hence, decay on a timescale of vibrational dephasing, which usually is in the order of a picosecond. It should be also noted that when vibrational frequency ω_0 matches the electronic energy gap ΔE_{MD} , the quantum mechanical mixing complicates the whole picture. Then damping of the resulting electronic-vibrational coherence will define the decay timescale of the oscillations in the spectra.

CONCLUSIONS

Coherent dynamics of coupled molecules can be effectively sorted out by the modeling of 2D spectra. Coupling between the multitude of vibrational states on different molecules results in a manifold of mixed states. When vibrational frequency and the electronic energy gap are off resonance this manifold constitutes two ladders of equally-spaced and well-resolved states. Two types of beats having either electronic or vibronic character can then be distinguished by the use of oscillation maps, constructed from the sequences of time-resolved 2D spectra.

We explicitly demonstrate effect of the inhomogeneous disorder on coherences of different character. The amplitude of the electronic-character beatings, caused by the coherences in excited states, is dramatically reduced by the disorder and consequently electronic coherences are quickly dephased. Vibrational-character beatings stem from ground and excited state contributions and depend weakly on the disorder, assuring their long-time survival.

We show that modeling of the oscillation maps observed in the experiments enables unraveling of the origin of the coherent beatings that is of direct relevance to their possible role for the energy and electron transfer processes in biological and artificial aggregates.

ACKNOWLEDGMENTS

This research was partially funded by the European Social Fund under the Global grant measure. V. B. acknowledges support by project "Promotion of Student Scientific Activities" (VP1-3.1-MM-01-V-02-003) from the Research Council of Lithuania. D. Z was supported by the Swedish Research Council.

* leonas.valkunas@ff.vu.lt

- [1] M. Pope and C. E. Swenberg. *Electron Processes in Organic Crystals*. Oxford University Press: New York/Oxford, 1999.
- [2] H. van Amerongen, L. Valkunas, and R. van Grondelle. *Photosynthetic Excitons*. World Scientific Co., Singapore, 2000.
- [3] A. S. Davydov. *Solitons in Molecular Systems*. Reidel, Dordrecht, 1985.
- [4] Jin Sun, Bin Luo, and Yang Zhao. Dynamics of a one-dimensional holstein polaron with the davydov ansatz. *Phys. Rev. B*, 82:014305, Jul 2010.
- [5] R-X. Xu, P. Cui, X-Q. Li, Y. Mo, and Y-J. Yan. Exact quantum master equation via the calculus on path integrals. *J. Chem. Phys.*, 122:041103, 2005.
- [6] Andrius Gelzinis, Darius Abramavicius, and Leonas Valkunas. Non-markovian effects in time-resolved fluorescence spectrum of molecular aggregates: Tracing polaron formation. *Phys. Rev. B*, 84:245430, Dec 2011.
- [7] S. Mukamel. Multidimensional femtosecond correlation spectroscopies of electronic and vibrational excitations. *Annu. Rev. Phys. Chem.*, 51:691–729, 2000.
- [8] D. M. Jonas. Two-dimensional femtosecond spectroscopy. *Annu. Rev. Phys. Chem.*, 54:425–463, 2003.
- [9] T. Brixner, J. Stenger, H. M. Vaswani, M. Cho, R. E. Blankenship, and G. R. Fleming. Two-dimensional spectroscopy of electronic couplings in photosynthesis. *Nature*, 434(7033):625–628, 2005.
- [10] D. Zigmantas, E. L. Read, T. Mančal, T. Brixner, A. T. Gardiner, R. J. Cogdell, and G. R. Fleming. Two-dimensional electronic spectroscopy of the B800-B820 light-harvesting complex. *Proc. Natl. Acad. Sci. USA*, 103(34):12672–12677, 2006.
- [11] G. S. Engel, T. R. Calhoun, E. L. Read, T. K. Ahn, T. Mančal, Y. C. Cheng, R. E. Blankenship, and G. R. Fleming. Evidence for wavelike energy transfer through quantum coherence in photosynthetic systems. *Nature*, 446:782, 2007.
- [12] E. Collini and G. D. Scholes. Coherent intrachain energy migration in a conjugated polymer at room temperature. *Science*, 323(5912):369–373, 2009.
- [13] Jaroslaw Sperling, Alexandra Nemeth, Jürgen Hauer, Darius Abramavicius, Shaul Mukamel, Harald F. Kauffmann, and Franz Miltot. Excitons and disorder in molecular nanotubes: A 2d electronic spectroscopy study and first comparison to a microscopic model. *J. Phys. Chem. A*, 114(32):8179–8189, 2010.
- [14] Joachim Seibt, Thorsten Hansen, and Tnu Pullerits. 3d spectroscopy of vibrational coherences in quantum dots: Theory. *J. Phys. Chem. A*, 0(0):null, 0.
- [15] T. R. Calhoun, N. S. Ginsberg, G. S. Schlau-Cohen, Y. C. Cheng, M. Ballottari, R. Bassi, and G. R. Fleming. Quantum coherence enabled determination of the energy landscape in light-harvesting complex II. *J. Phys. Chem. B*, 113:16291–16295, 2009.
- [16] Sebastian Westenhoff, David Paleček, Petra Edlund, Philip Smith, and Donatas Zigmantas. Coherent picosecond exciton dynamics in a photosynthetic reaction center. *J. Am. Chem. Soc.*, 134(40):16484–16487, 2012.
- [17] V. Butkus, D. Zigmantas, L. Valkunas, and D. Abramavicius. Vibrational vs. electronic coherences in 2D spec-

trum of molecular systems. *Chem. Phys. Lett.*, 545:40–43, 2012.

[18] Vivek Tiwari, William K. Peters, and David M. Jonas. Electronic resonance with anticorrelated pigment vibrations drives photosynthetic energy transfer outside the adiabatic framework. *Proc. Natl. Acad. Sci. USA*, 110(4):1203–1208, 2013.

[19] Tomáš Mančal, Niklas Christensson, Vladimír Lukeš, Franz Milota, Oliver Bixner, Harald F. Kauffmann, and Jürgen Hauer. System-dependent signatures of electronic and vibrational coherences in electronic two-dimensional spectra. *J. Phys. Chem. Lett.*, 3(11):1497–1502, 2012.

[20] A. W. Chin, J. Prior, R. Rosenbach, F. Caycedo-Soler, S. F. Huelga, and M. B. Plenio. The role of non-equilibrium vibrational structures in electronic coherence and recoherence in pigment-protein complexes. *Nature Phys.*, 9(2):113–118, February 2013.

[21] Niklas Christensson, Harald F. Kauffmann, Tõnu Pullerits, and Tomáš Mančal. Origin of long-lived coherences in light-harvesting complexes. *J. Phys. Chem. B*, 116(25):7449–7454, 2012.

[22] Vytautas Butkus, Leonas Valkunas, and Darius Abramavicius. Molecular vibrations-induced quantum beats in two-dimensional electronic spectroscopy. *J. Chem. Phys.*, 137(4):044513, 2012.

[23] T. Mančal, A. Nemeth, F. Milota, V. Lukeš, H. F. Kauffmann, and J. Sperling. Vibrational wave packet induced oscillations in two-dimensional electronic spectra. ii. theory. *J. Chem. Phys.*, 132:184515, 2010.

[24] D. Abramavicius, V. Butkus, J. Bujokas, and L. Valkunas. Manipulation of two-dimensional spectra of excitonically coupled molecules by narrow-bandwidth laser pulses. *Chem. Phys.*, 372(1-3):22–32, 2010.

[25] D. Abramavicius, L. Valkunas, and S. Mukamel. Transport and correlated fluctuations in the nonlinear optical response of excitons. *Europhys. Lett.*, 80(1):17005, 2007.

[26] Jakub Dostál, Tomáš Mančal, Ramūnas Augulis, František Vácha, Jakub Pšenčík, and Donatas Zigmantas. Two-dimensional electronic spectroscopy reveals ultrafast energy diffusion in chlorosomes. *J. Am. Chem. Soc.*, 134(28):11611–11617, 2012.

[27] Gabriela S. Schlau-Cohen, Tessa R. Calhoun, Naomi S. Ginsberg, Elizabeth L. Read, Matteo Ballottari, Roberto Bassi, Rienk van Grondelle, and Graham R. Fleming. Pathways of energy flow in lhcii from two-dimensional electronic spectroscopy. *J. Phys. Chem. B*, 113(46):15352–15363, 2009.